MICHIGAN STATE UNIVERSITY

CYCLOTRON LABORATORY

M1 EXCITATION OF NUCLEI BY INELASTIC PROTON SCATTERING

N. ANANTARAMAN, G.M. CRAWLEY, A. GALONSKY, C. DJALALI, N. MARTY, M. MORLET, A. WILLIS, J.-C. JOURDAIN and P. KITCHING

Second Indo-U.S. Joint Symposium on

NUCLEAR PHYSICS AT CYCLOTRON AND INTERMEDIATE ENERGIES

May 24-28, 1982

Bombay, India

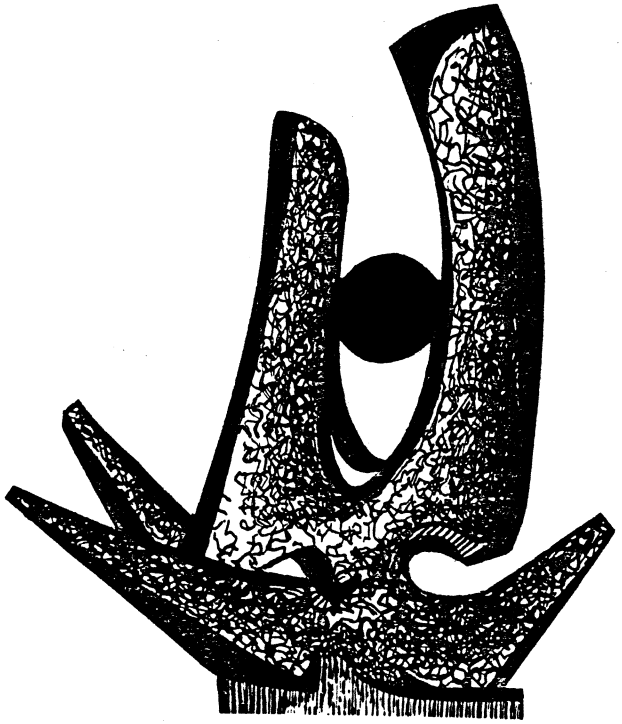

MAY 1982

MSUCL-374

INVITED TALK AT SECOND INDO-U.S. SYMPOSIUM ON NUCLEAR PHYSICS AT CYCLOTRON AND INTERMEDIATE ENERGY, BOMBAY, MAY 24-28, 1982.

M1 EXCITATION OF NUCLEI BY INELASTIC PROTON SCATTERING

N. ANANTARAMAN, G.M. CRAWLEY and A. GALONSKY
National Superconducting Cyclotron Laboratory,
Michigan State University
East Lansing, Michigan 48824
and
C. DJALALI, N. MARTY, M. MORLET, A WILLIS,
J.-C. JOURDAIN and P. KITCHING
Institut de Physique Nucléaire
Orsay, France

Abstract

The giant M1 excitation has been observed in the inelastic scattering of 200-MeV protons from 23 medium-heavy nuclei between ^{40}Ca and ^{140}Ce. The M1 identification is based upon the excitation energies (between 8 and 9 MeV in most of the nuclei) and angular distributions (very forward peaked) of structures observed in the proton spectra. Microscopic distorted wave impulse approximation calculations match the shapes of the angular distributions quite well but predict cross sections about 4 times too large. Comparisons with (e,e') and (p,n) results are presented.

I. Introduction

The study of M1 excitation gives information on the nuclear spin degrees of freedom, whose exploration is currently one of the most active areas of research in nuclear physics, as was demonstrated by the recent conference at Telluride on this subject[1]. The excitation of this spin-flip transition requires special properties of the probe, unlike the excitation of natural parity levels. Two probes that have proved to be very selective are the (p,n) reaction at high energies[2] and inelastic electron scattering at back angles[3]. The high-

energy (p,p') work which is discussed in this paper was stimulated by the results from these other reactions and complements them in the following ways:

(1) Electron scattering has contributions from both orbital and spin parts, whereas only the latter contributes in (p,p') at low momentum transfer (forward angles). Thus a comparison will allow separation of the two parts[4].

(2) The M1 states excited in (e,e') are accompanied by a huge background of M2 states. In heavy nuclei, where it is difficult to get to low enough momentum transfer to identify M1 states clearly, there is then the possibility of a $J^\pi = 1^+, 2^-$ ambiguity. In (p,p'), on the other hand, it is straightforward to establish a L=0 shape for the angular distribution. Thus the J^π ambiguity in (p,p') is between 0^+ and 1^+, corresponding to $\Delta S = 0$ and 1, respectively. By comparing the results from the two reactions, therefore, one can pick out the 1^+ states.

(3) The strength in a (p,n) reaction is a measure of the neutron excess (N-Z), while the (p,p') strength is sensitive to spin pairings among the nucleons. Thus the strengths measured in the two reactions could be different.

(4) The (p,p') reaction has typically a much better resolution than (p,n), (70 keV compared with 400 keV), which aids in the identification of states.

Another motivation for the (p,p') work was a long-standing puzzle[5], viz. the non-observation of substantial M1 strength in nuclei heavier than Ni in both (e,e') and (p,p'). In a simple shell model, one would expect appreciable M1 strength in a spin-unsaturated nucleus, viz one in which the $j_> = \ell + 1/2$ level is occupied, while the $j_< = \ell - 1/2$ level is empty. An example of such a nucleus is ^{90}Zr, where the $g_{9/2}$ orbit is filled with neutrons while the $g_{7/2}$ orbit is empty. Spin pairings in the nucleus would lead to partial occupancy of the $j_<$ level in the ground state, thereby reducing the M1 strength, but the basic picture would be unchanged. Thus the non-observation of M1 strength was a major problem.

Two clues to the search for the M1 state in the Zr isotopes were provided by the results of high-energy (p,n) reaction on

these nuclei. In Fig. 1 is shown the 0^{o} spectrum for ^{90}Zr at a bombarding energy of 120 MeV[6]. The dominance of the 1^{+} levels relative to the 0^{+} isobaric analogue state was found to increase as the bombarding energy was raised. This has been understood in terms of the different energy dependences of the different components of the effective interaction between the projectile and target nucleons[7]. The same feature should be present for (p,p'), since the reaction kinematics would be the same for both (p,p') and (p,n). That was the first clue: an indication of the kinematic region to be investigated, viz a high bombarding energy (>100 MeV) and very forward angles. A second clue was regarding the excitation of the state in ^{90}Zr. That came about because the small 1^{+} peak in the (p,n) spectrum located about 8 MeV above the isobaric analogue state was identified as the analogue of the parent M1 state. This implied that the parent state in ^{90}Zr would also be at about 8 MeV excitation.

These considerations led to a program of studying M1 strength in medium-heavy nuclei by the inelastic scattering of 200-MeV protons, in a collaborative effort between groups from Michigan State University and I.P.N., Orsay at the Orsay synchrocyclotron that began in early 1981. To date, we have studied (in varying detail) 23 nuclei ranging from ^{40}Ca to ^{140}Ce[8-10].

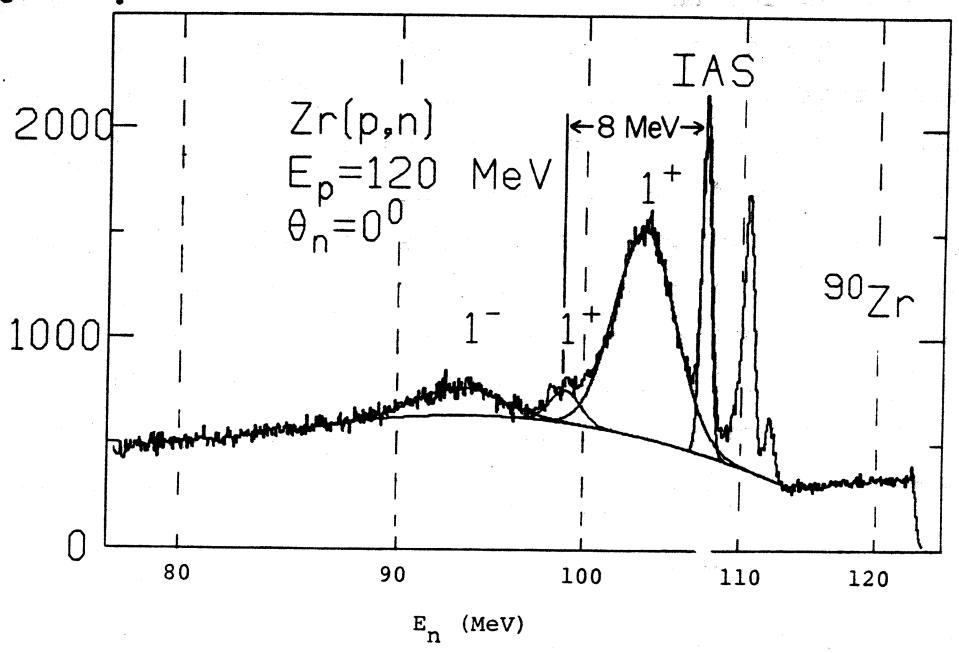

FIG. 1. The spectrum of neutrons in the reaction $^{90}Zr(p,n)$ at 120 MeV (ref. [6]).

2. Experimental Method

The requirement of a high proton energy, coupled to the ability to measure inelastic scattering spectra at very forward angles with very low background, is experimentally nontrivial. The system[11] at the Orsay synchrocyclotron meets this requirement almost ideally. The key feature of the detection system is the ability to measure trajectories of scattered particles by means of two position sensitive proportional counters. By setting an angular window on the trajectories, the background due to slit-scattered particles is reduced significantly. But the counter system had a small differential nonlinearity, which produced spurious fine structure in the spectrum corresponding to certain positions along the wires. We overcame this by measuring each spectrum twice, with two slightly different settings of the magnetic field, and comparing their overlap.

3. Results

3.1 ^{40}Ca: A TEST CASE

The nucleus ^{40}Ca, where a discrete 1^+ level at 10.3 MeV was already known from (e,e') work[12], was first studied to test our experimental technique. This level is clearly seen in the 3^o (p,p') spectrum (Fig. 2), where it is one of the few states selectively excited. But by 7^o it has almost disappeared into the background of other levels. The reason for this is that the Ml states are excited predominantly by an angular momentum transfer L of zero, which has a very forward-peaked angular distribution (Fig. 3). Also shown in Fig. 3 is the angular distribution for the 2^- level at 8.43 MeV, which is excited mainly by L=1. It is evident that the L=0 and L=1 angular distributions are quite different, so that it is easy to establish the L=0 shape associated with the Ml states.

3.2 THE EVEN Zr ISOTOPES

Figure 4 shows the 4^o spectra for ^{90,92,94,96}Zr. The broad bump centered at about 16 MeV excitation is probably a mixture of the giant dipole, quadrupole and monopole

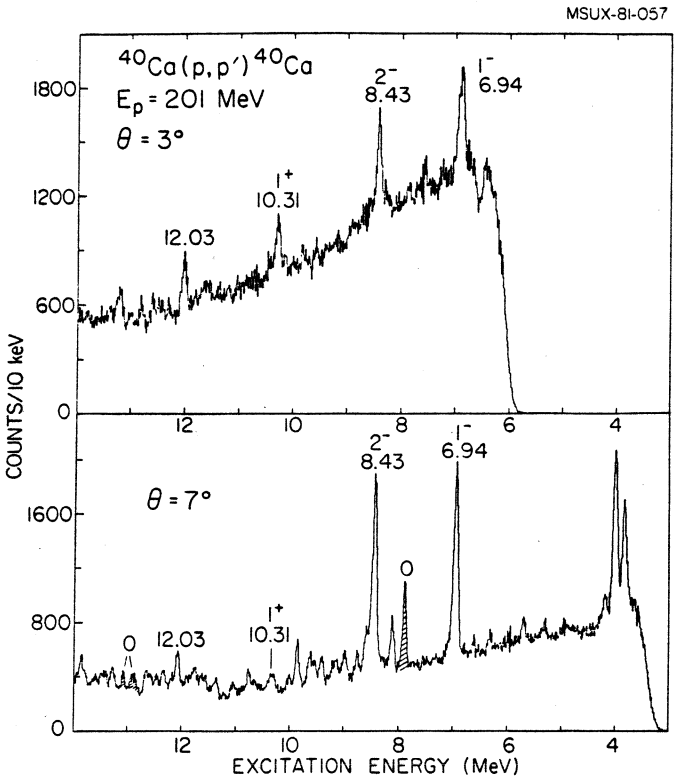

FIG. 2. Spectra of protons inelastically scattered from ^{40}Ca at 3° and 7°. Peaks due to an oxygen containminant are shown hatched.

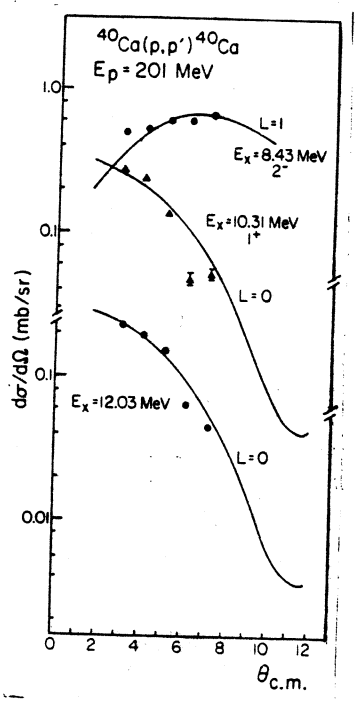

FIG. 3. Angular distributions for a number of states in ^{40}Ca. The state at 12.03 MeV was previously unknown.

resonances. This will not be discussed further. What is of interest to us is the broad bump indicated by the arrows, which we identify as the M1 resonance in the Zr isotopes. This peak occurs at an excitation of about 9 MeV in all four nuclei; it has a full width at half maximum of about 1.5 MeV; its shape varies from isotope to isotope and is neither smooth nor symmetric. The dashed curves show the background that was used to extract the yield.

For ^{90}Zr, the M1 state was also observed in another (p,p') experiment at 200 MeV, performed at TRIUMF[13]. It has features similar to those present in our spectra.

The M1 identification is based upon the following. First, the peak has a L=0 angular distribution (Fig. 5). This is established in two ways: (a) By comparing the measured shape

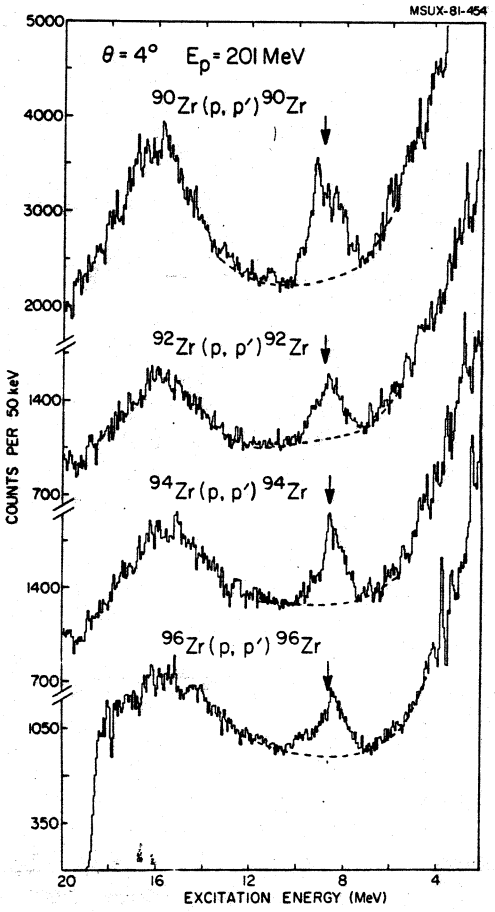

FIG. 4. Spectra of protons inelastically scattered from ^{90}Zr, ^{92}Zr, ^{94}Zr and ^{96}Zr at 4°. The arrows indicate the centroids of the M1 resonance.

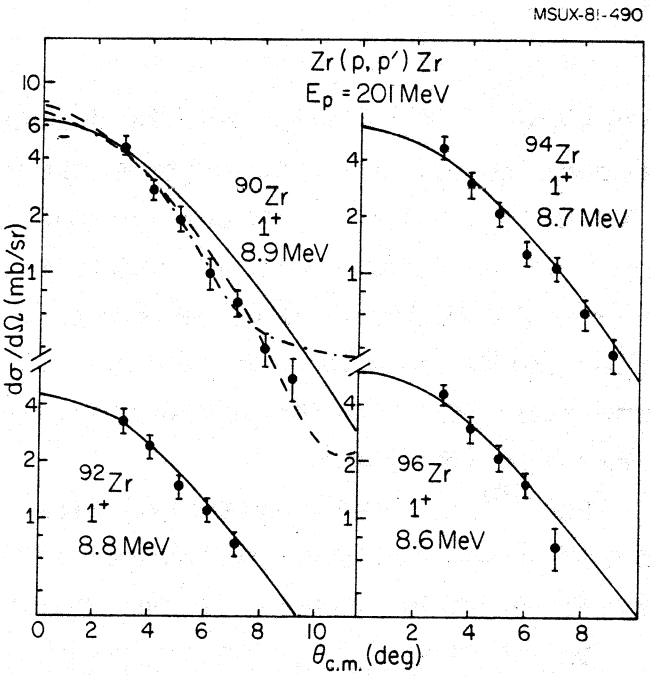

FIG. 5. Angular distributions for the M1 resonance in the even Zr isotopes. The solid and dashed curves are DWIA predictions, normalized to the data. The curve shown for ^{96}Zr is the calculation for ^{90}Zr. The dot-dashed curve is from a $^{90}Zr(p,n)$ measurement (ref. [14]).

with that predicted by a microscopic distorted wave impulse approximation (DWIA) calculation, shown by the solid curves; (b) By comparing with the experimental ^{90}Zr(p,n) angular distribution measured at 200 MeV[14], shown by the dot-dashed curve. It is seen that all four nuclei have the same angular distribution shape.

Now, a L=0 shape implies $J^\pi = 0^+$ or 1^+. One can distinguish between these two possibilities by studying the bombarding energy dependence of the cross section, since the $1^+/0^+$ ratio would increase with the energy. In a study[15] of the ^{90}Zr(p,p') reaction several years ago at E(p) = 24 MeV, no structure was found around 9 MeV excitation. That is part of our argument for the M1 identification. Another part is the agreement between the measured excitation energy and that expected from the (p,n) reaction, where the analogue of this state has been observed. (See Fig. 1.)

The next question is: how strongly is the M1 state excited? We answer it by comparing the measured cross section with that predicted by a microscopic DWIA calculation. One of the key ingredients required in the DWIA calculation is the wave function, or more precisely the transition amplitudes, for the 1^+ states. This requires a detailed shell-model calculation. For ^{90,92,94}Zr, Anantaraman and Wildenthal have done such a calculation[16]. The same could not be done for ^{96}Zr because the dimensionality became too large. Briefly, this model considers only neutron excitations and, in the case of ^{90}Zr, is identical with the simplest model for the 1^+ level, viz. $\nu g_{7/2} g_{9/2}^{-1}$. The calculated B(M1) strength distribution is shown in Fig. 6. Note that the calculation finds a concentration of M1 strength at a particular excitation energy, as in the data, rather than spread out over all excitations. Again, as in the data, the excitation energy is the same for all three nuclei, though it is located about 1 MeV lower than observed.

Incidentally, there will not in general be a strict correspondence between B(M1) values and (p,p') cross sections, because there are both orbital and spin contributions in the former, while only the spin part contributes in the latter. But in cases where only neutron excitations are involved, such

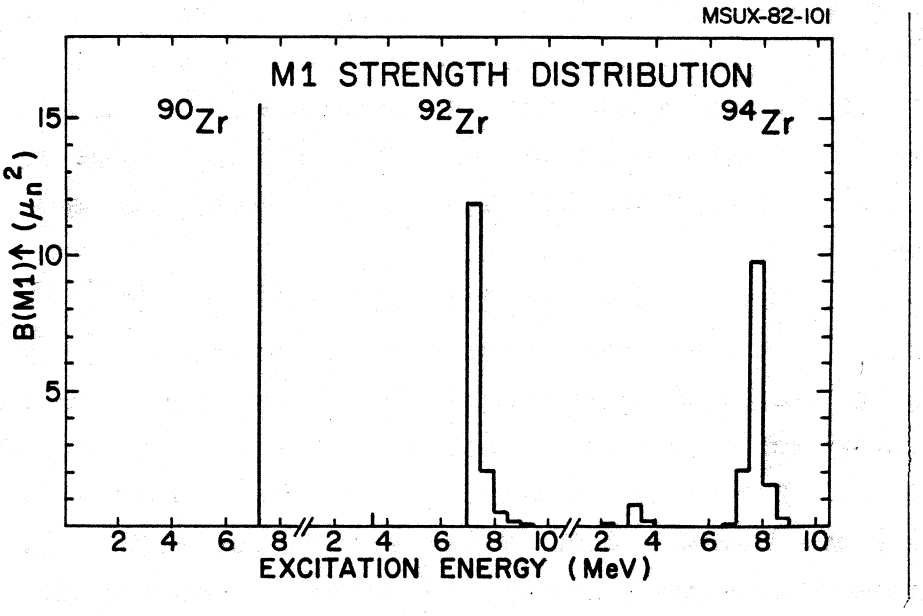

FIG. 6. Calculated B(M1) strength distribution in ^{90,92,94}Zr (ref. [15]).

as the Zr isotopes, there is no orbital part to B(M1) and there is a strict correspondence between B(M1) values and (p,p') cross sections.

The comparison between the data and the DWIA calculations (done with the code DWBA70) is shown in Table 1. The 4° cross sections measured for all four nuclei are the same within error bars. So also are the calculated cross sections (no

Table 1

Cross sections to the M1 state measured and calculated for the Zr(p,p')Zr reaction at E(p) = 201 MeV

Nucleus	$\sigma_{exp}(4^{\circ})$ mb/sr	$N = \sigma_{exp}/\sigma_{calc}$
^{90}Zr	2.8 ± 0.4	0.26
^{92}Zr	2.5 ± 0.4	0.19
^{94}Zr	3.0 ± 0.4	0.26
^{96}Zr	3.0 ± 0.4	--

calculation for ^{96}Zr because of the lack of transition amplitudes). This leads to a constant normalization $N = \sigma_{exp}/\sigma_{calc}$ of 0.25 ± 30% for all the nuclei. This error takes account of the uncertainties in the measured and calculated cross sections and the lack of a perfect fit of the calculated angular distribution to the data.

Ideally, one would expect a value of unity for N. The departure of N from 1 is the famous quenching of M1 transitions [17], which has been attributed to two causes: (1) configuration mixing (in particular, spin pairing) and (2) mesonic effects, in particular the mixing of Δ-N^{-1} configurations with the M1 state. Typically, calculations find a 25% reduction of strength due to (1) and a 30-35% reduction due to (2). The first effect is already partly included in the above N, for ^{92}Zr and ^{94}Zr. ("Partly", because a restricted model space was used in the shell-model calcualtion; it decreased the ^{94}Zr strength by 25%. A larger space would have produced a larger decrease.) The second effect can be included by renormalizing the spin operator such that the magnetic moment of the ground state of ^{91}Zr is correctly reproduced. This method is, however, open to debate because it implicitly assumes that the mesonic correction is state independent. Such a renormalization changes the above N from 0.25 to 0.39, which is to be compared with the expected value of unity.

The value of N = 0.25 is to be compared with N = 0.50 obtained from the ^{90}Zr(p,n) data[18]. It is important to point out that the (p,n) value is not for the analogue of the M1 state but for the total Gamow-Teller strength, of which the analogue state forms only a small part. Thus there is no state-to-state correspondence between the (p,p') and (p,n) values. Still, the difference in the two N values is interesting. A possible reason for it is the occurrence of spin pairings among the excess neutrons over and above those included in the model of ref. [16]. Such pairings will decrease the (p,p') strength but leave the (p,n) strength unaffected.

Finally, while the M1 strength found in a high-resolution (e,e') study[19] of ^{90}Zr occurs at approximately the same excitation energy as found in (p,p'), the distributions of strength in the two reactions bear little resemblance. The

(e,e') measurement finds most of the M1 strength in three discrete levels, quite unlike the broad peak found by us. The reason for this is unknown and it remains a major puzzle. One would have expected good agreement between the two measurements in the case of ^{90}Zr, since only neutron excitations are involved. The total M1 strength found in (e,e') is 25% of the expected strength, just as in (p,p'), but this agreement is probably fortuitous.

4. Survey of M1 Systematics

In Fig. 7 are shown the 4^{o} spectra for the even Mo isotopes. The M1 resonance is the gross-structure enhancement centered at 8 to 10 MeV. The location of the peak in the valley between two hills makes its identification relatively easy. In contrast, in the three heaviest nuclei we have studied--^{120}Sn, ^{124}Sn and ^{140}Ce-the elastic tail is so prominent that the M1 peak lies on the hillside and is correspondingly more difficult to analyze (Fig. 8). These mass 120-140 nuclei probably represent the limits to which the search for M1 strength can be pushed with our present technique.

The near constancy of the M1 excitation energy over the range of nuclei studied is shown in Fig. 9, where the centroid of the M1 peak is plotted as a function of A. This constancy is easy to understand in a simple picture. The excitation energy is determined primarily by the splitting of the spin-orbit partner levels involved in the transition, increased by a few MeV due to the repulsive particle-hole interaction. Since neither of these effects is expected to have much A dependence, the M1 energy would also be nearly mass independent.

In Table 2, the M1 strengths extracted for some of these nuclei are listed. Only those nuclei were considered for which it was felt that the simple 1^{+} wave functions shown were not too bad an approximation. (One of the chief factors preventing full analysis of our data is the lack of detailed shell-model calculations for most of the nuclei studied.) The strengths extracted with the simple wave functions are about 25% of the expected values and seem to be A-independent. The A-independence is also seen in the (p,n) data[18], but the value

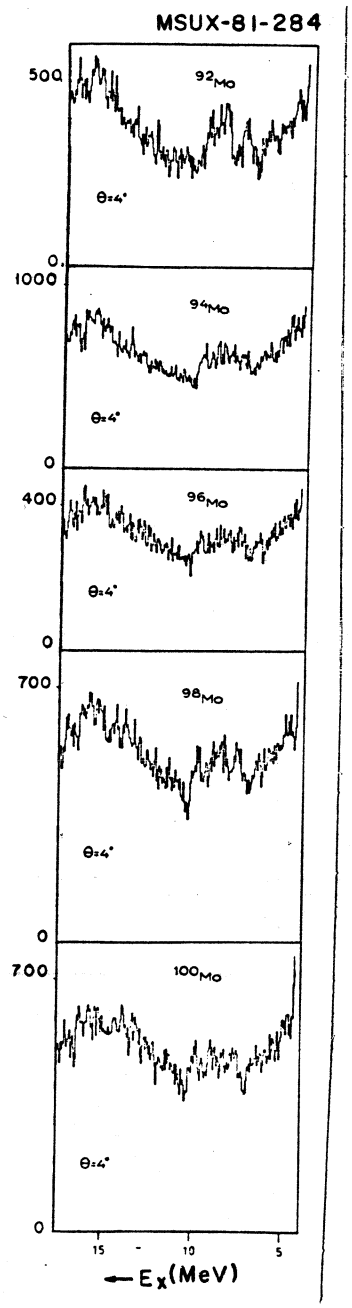

FIG. 7. Spectra of protons inelastically scattered from the even Mo iostopes at 4^{o}.

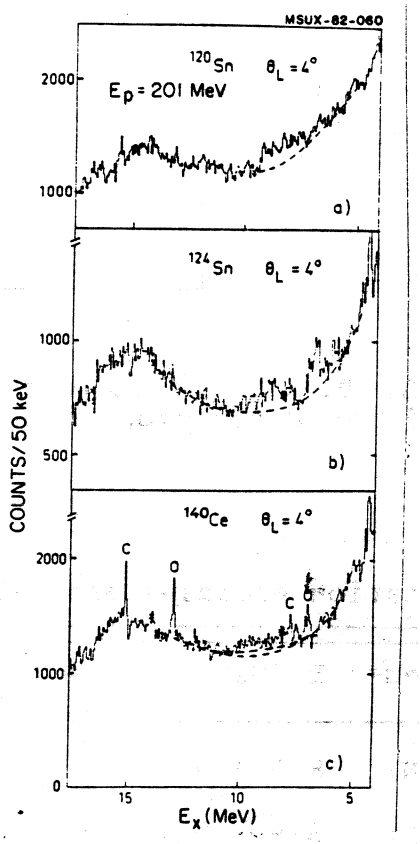

FIG. 8. Spectra of protons inelastically scattered from ^{120}Sn, ^{124}Sn and ^{140}Ce at 4^{o}. The dashed lines indicate backgrounds assumed in extracting peak areas. Two choices are shown for ^{140}Ce.

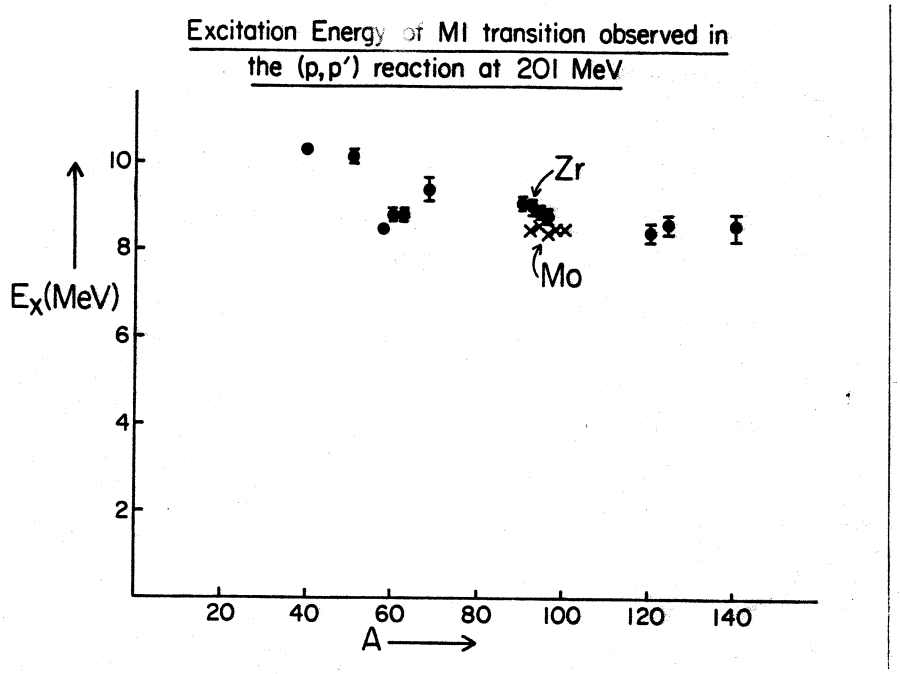

FIG. 9. Centroid energy of the M1 resonance observed in (p,p') as a function of mass number.

Table 2

Excitation energies and strengths for ^{1}M1 states

Nucleus	E_x(MeV)	$N = \sigma_{exp}/\sigma_{calc}$	1^+ Wave Function
^{58}Ni	8.5 ± 0.1	0.22	$\frac{1}{\sqrt{2}}\left[\pi(f_{5/2}f_{7/2}^{-1})-\nu(f_{5/2}f_{7/2}^{-1})\right]$
^{90}Zr	8.9 ± 0.2	0.26	$\nu(g_{7/2}g_{9/2}^{-1})$
^{92}Mo	8.5 ± 0.2	0.21	$\nu(g_{7/2}g_{9/2}^{-1})$
^{120}Sn	8.4 ± 0.2	0.21	$\pi(g_{7/2}g_{9/2}^{-1})$

of N there is two times as large. As in the case of the Zr isotopes, a possible reason for this difference is the occurrence of ground-state spin pairings in these nuclei.

5. The Even Ni Isotopes: Striking Isospin Features

In Fig. 10 are shown the 4^{o} spectra for ^{58,60,62,64}Ni. There are two prominent features in each spectrum: the by-now

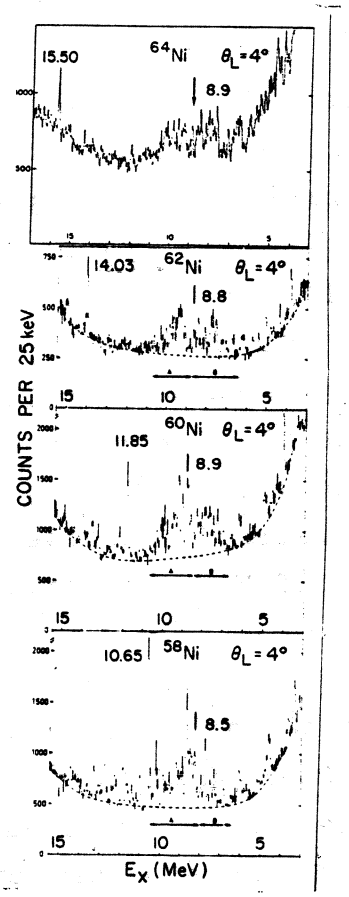

FIG. 10. Spectra of protons scattered from ^{58,60,62,64}Ni at 4°. The centroids of the broad bumps are shown by arrows and excitation energies are indicated in MeV.

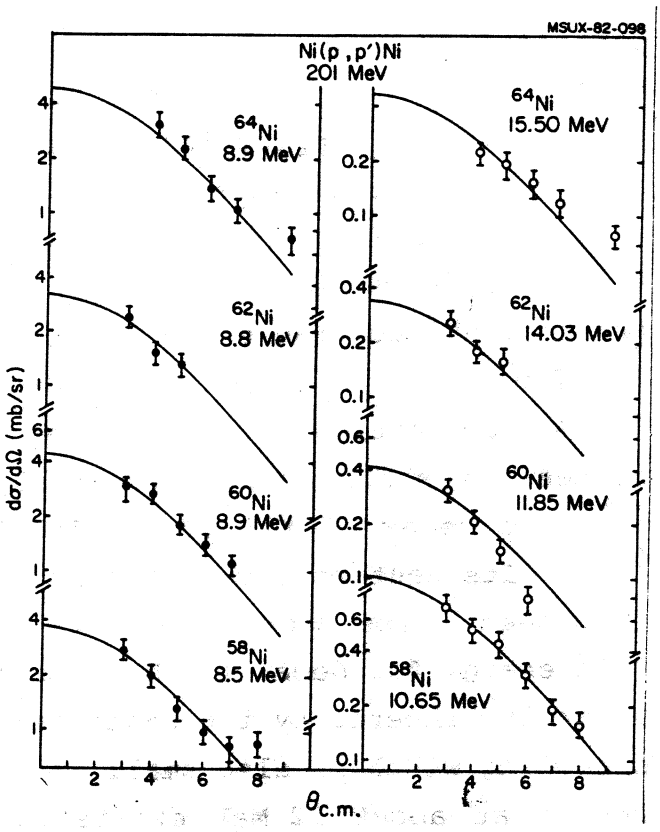

FIG. 11. Angular distributions for the broad bumps (left) and sharp peaks (right) in the Ni isotopes. The solid curve is a DWIA calculation individually normalized for each case.

familiar broad bump around 9 MeV excitation and a sharp peak at a higher excitation energy. The sharp peak moves to increasingly higher excitation as the mass of the nucleus increases. In ^{64}Ni, the peak is at 15.5 MeV excitation and yet it has a width smaller than the experimental resolution. We identify the broad peak as the T_0 component of the M1 resonance and the sharp peak as a part of the (T_0+1) component, where T_0 is the target isospin. Note that in the Zr isotopes there was

no (T_0+1) component, because only neutron excitations were involved. But in the Ni isotopes, both neutrons and protons contribute to the M1 transition, because the $f_{7/2}$ orbit is filled with both protons and neutrons in the ground states of these nuclei. Appropriate linear combinations of the proton and neutron excitations lead to the T_0 and (T_0+1) components.

This identification explains all our observations. Figure 11 shows the angular distributions for the broad peak on the left and for the sharp peak on the right, respectively, for the four nuclei. They are characteristic of L=0, as required for M1 transitions. It is also easy to see why the (T_0+1) states are sharp despite their high excitation. Consider the particle decay of the (T_0+1) level at 11.85 MeV excitation in ^{60}Ni. Its neutron decay to the ground state of ^{59}Ni is isospin forbidden. Its proton decay to ^{59}Co is energetically allowed (the energy for decay to the ground state being 2.3 MeV) but is strongly hindered by the centrifugal and Coulomb barriers. Its spreading width is also small, because the density of (T_0+1) 1^+ levels at about 12 MeV excitation in ^{60}Ni is expected to be small. Thus the total width of the level is small, leading to its sharpness.

The increasing separation between the T_0 and (T_0+1) components with increasing mass is also readily understood in terms of the isospin splitting relation,

$$\Delta E = E_{T_0+1} - E_{T_0} = \frac{V_1}{A} (T_0+1),$$

where V_1 is the depth of the symmetry potential. (This formula assumes that the two components have the same structure, which may be open to question.) The isospin T_0 increases from 1 for ^{58}Ni to 4 for ^{64}Ni. The value of V_1 deduced from our data is 82.5 MeV for ^{58}Ni, 74.5 MeV for ^{60}Ni, 81.1 MeV for ^{62}Ni and 84.5 MeV for ^{64}Ni. (In the case of ^{58}Ni and ^{60}Ni, all the smaller fine structure at high excitation was included in the (T_0+1) component when obtaining the above V_1 values.) These values agree nicely with the value of 85 MeV obtained from (p,n) systematics[20].

In the case of ^{58}Ni, the M1 levels have also been excited by (e,e'), both by Lindgren et al.[21] and by Richter et al.[22].

Figure 12 shows a comparison between our data and the data of ref. 22) for the (T_0+1) levels. The (p,p') and (e,e') cross sections have been normalized to each other for the strongest of these levels. The excitation energies found in the two reactions for the different levels are in agreement. There are some differences in the relative strengths found, which might be accounted for in terms of the orbital contribution present in (e,e') but absent in (p,p'). A quantitative analysis of these differences will shed light on the wave functions of the states excited.

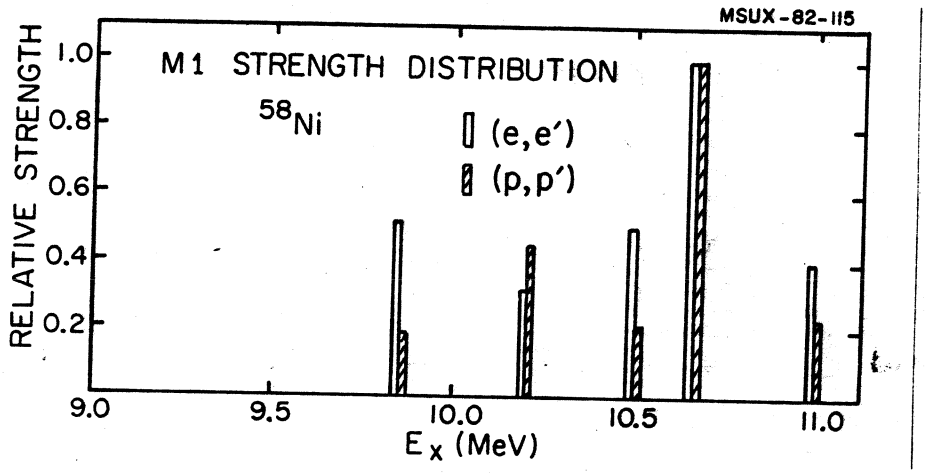

FIG. 12. Comparison between (p,p') and (e,e') (ref. 22)) cross sections for (T_0+1) levels in ^{58}Ni.

6. N=28 Isotones

6.1. ^{48}Ca: A MAGIC NUCLEUS

The spectra measured at forward angles are shown in Fig. 13. The famous 1^+ level at 10.2 MeV, first seen in electron scattering[12], completely dominates the spectrum at forward angles. By 8^o, other levels of higher multipolarities begin to appear. The angular distribution for the 10.2 MeV level is shown in Fig. 14. The dashed curve is the result of a microscopic calculation using the simplest wave function for the 1^+ state, while the full curve uses the full fp-shell wave function[23]. The two curves have been individually normalized to the data. The fit to the measured shape is acceptable but poorer than for some of the other nuclei discussed before.

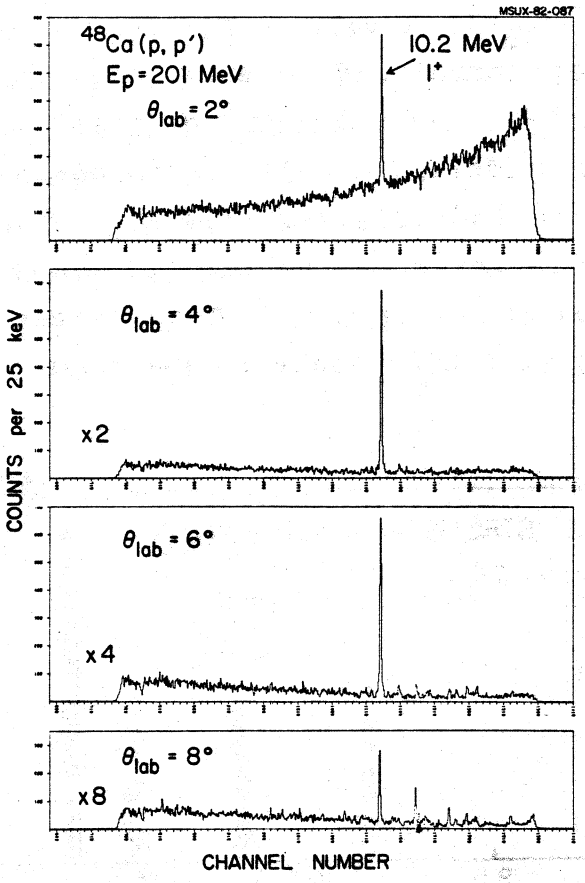

FIG. 13. Spectra from the ^{48}Ca(p,p') reaction.

The normalizations N obtained with the different calculations are given in Table 3. The left column gives the results from (p,p'), while the right column gives the (e,e') results. The full fp-shell result includes the effect of spin pairings in the ground state. The number in the last row uses a renormalized value of the spin operator σ which reproduces[23] the experimental magnetic moment of ^{41}Ca. Thus this number includes the effect of ground-state correlations as well as the mesonic effect--though (as stated before) in a way that may be open to debate. At this stage, one would have expected to find a N of unity, since both quenching mechanisms have been taken into account. Instead, we find a value close to 0.5. The value of N obtained from (e,e') agrees with this within the uncertainties: $\pm$25% in the (p,p') value, $\pm$10% in the (e,e') value.

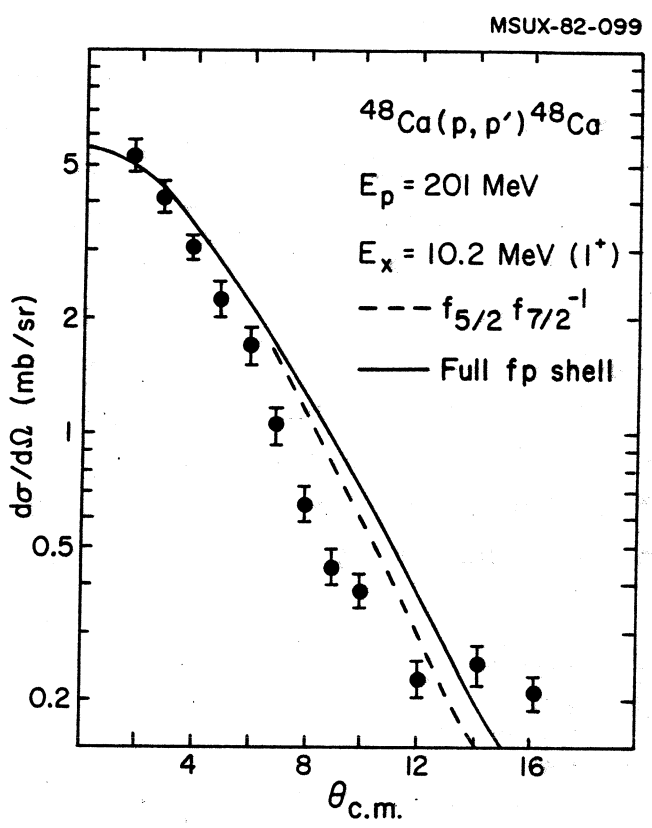

FIG. 14. Angular distribution for the 10.2 MeV 1^+ level observed in $^{48}Ca(p,p')$.

Table 3

Strength of the 1^+ (10.2 MeV) level in ^{48}Ca

Model Used	$N = \sigma_{exp}/\sigma_{calc}$ from (p,p')	$N' = B_{exp}(M1)/B_{calc}(M1)$ from (e,e')
$f_{5/2}f_{7/2}^{-1}$	0.27	0.33
Full fp-Shell	0.36	0.47
Renormalized σ	0.52	0.68

6.2 RESULTS FOR ^{50}Ti, ^{51}V, ^{54}Fe

The (p,p') spectra measured for ^{50}Ti and ^{54}Fe are shown in comparison with the ^{48}Ca spectrum in Fig. 15. We see here the effect of adding successive pairs of protons in the $f_{7/2}$ shell to the ^{48}Ca core. The one strong neutron-excitation level in ^{48}Ca splits up into many levels in ^{50}Ti and into even more levels in ^{54}Fe. The centroid of the neutron excitations is however remarkably constant in the three nuclei. What may be loosely called proton excitations occur at somewhat lower energies. These results agree qualitatively with those[24] from (e,e'). However, in ^{51}V, whereas the (p,p') data show a broad peak near 10.2 MeV (Fig. 16), the (e,e') data show no strength at all! This mystery remains to be cleared up. We find that

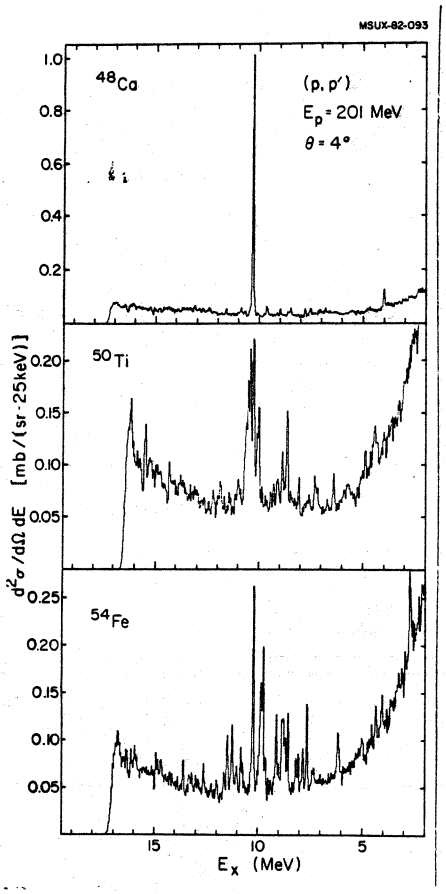

FIG. 15. Spectra of protons scattered from ^{48}Ca, ^{50}Ti and ^{54}Fe.

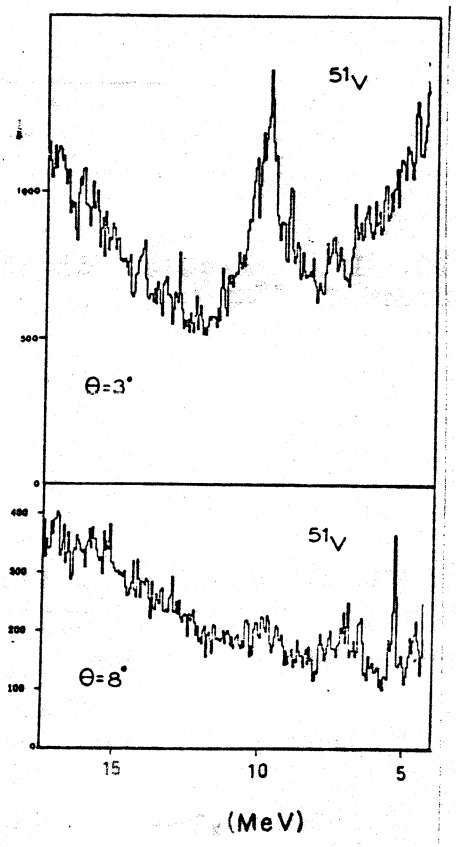

FIG. 16. Spectra of protons scatte from ^{51}V at 3^{o} and 7^{o}.

the total M1 strength is same in ^{50}Ti and ^{54}Fe, being about 60% larger than in ^{48}Ca. A shell-model calculation by Knüpfer and Metsch reproduces this trend quantitatively[24]. A detailed comparison with their results remains to be done.

7. Summary

M1 states have been excited in 23 medium-heavy nuclei between ^{40}Ca and ^{140}Ce by the inelastic scattering of 200-MeV protons. The states have an excitation energy of about 9 MeV in most of the nuclei, with a width of about 1.5 to 2 MeV. The value of the excitation energy as well as its approximate A-independence are understandable in a simple picture. The strength extracted is about 0.25 of the expected strength and it seems to be A-independent, although more detailed structure calculations are needed to establish the precise value of this quenching. For comparison, the strength found in (p,n) reactions is about 0.5. Comparison with (p,n) and (e,e') results shows up areas of agreement as well as areas of disagreement. A quantitative analysis of these differences should shed additional light on the structure of the 1^+ states. Thus the interaction between different experimental methods is proving very fruitful in understanding M1 transitions in nuclei.

Acknowledgements

This work was partly supported by the U.S. National Science Foundation under Grant No. Phy-78-22696. Three of the authors (NA, GMC and AG) received travel support from the INT Division of the National Science Foundation. The authors are indebted to H. Toki, W.G. Love, N. Auerbach, Nguyen Van Giai, D. Gogny and J. Decharge for many enlightening discussions.

References

1. Proc. Int. Conf. on Spin Excitations in Nuclei, Telluride, 1982, ed. F. Petrovich.
2. C.D. Goodman, Nucl. Phys. A374 (1982) 241.

3. A. Richter, Nucl. Phys. A374 (1982) 177.
4. F. Petrovich, W.G. Love and R.J. McCarthy, Phys. Rev. C21 (1980) 1718.
5. G.F. Bertsch, L. Zamick and A. Mekjian, in Lecture Notes in Physics, Vol. 119 (Springer-Verlag, New York, 1980), p. 245.
6. W. Sterrenburg et al., in Proc. Int. Conf. on Nuclear Structure, Berkeley, 1980, (Abstracts), p. 176.
7. W.G. Love and M.A. Franey, Phys. Rev. C24 (L981) 1073.
8. N. Anantaraman et al., Phys. Rev. Lett. 46 (1981) 1318.
9. G.M. Crawley et al., Phys. Rev. C, to be published.
10. C. Djalali et al., Nucl. Phys. A, to be published.
11. A. Willis et al., Nucl. Phys. A344 (1980) 137.
12. W. Steffan et al., Phys. Lett. 95B (1980) 23.
13. F.E. Bertrand et al., Phys. Lett. 103B (1981) 326.
14. C. Gaarde et al., Nucl. Phys. A369 (1981) 258.
15. F.E. Cecil, G.T. Garvey and W.J. Braithwaite, Nucl. Phys. A232 (1974) 22.
16. N. Anantaraman and B.H. Wildenthal, to be published.
17. A. Arima and H. Hyuga, in Mesons in Nuclei, ed. M. Rho and D.H. Wilkinson, (North-Holland, Amsterdam, 1979), Vol. II, p. 683; M. Rho, Nucl. Phys. A231 (1974) 493; A. Bohr and B.R. Mottelson, Phys. Lett. 100B (1981) 10.
18. C.D. Goodman and C. Gaarde, in ref. 1; and priv. comm.
19. D. Meuer et al., Nucl. Phys. A349 (1980) 309.
20. W. Sterrenburg et al., Phys. Rev. Lett. 45 (1980) 1839.
21. R.A. Lindgren et al., Phys. Rev. C14 (1976) 1789.
22. A. Richter, in Proc. Int. School on Nuclear Structure, Alushta, USSR, 1980, p. 89; and priv. comm.
23. J.B. McGrory and B.H. Wildenthal, Phys. Lett. 103B (1981) 173.
24. A. Richter, priv. comm.